Cancer Letters 448 (2019) 155–167

Contents lists available at ScienceDirect

Cancer Letters

journal homepage: www.elsevier.com/locate/canlet

Original Articles

# Essential role of JunD in cell proliferation is mediated via MYC signaling in prostate cancer cells

Bethtrice Elliott[a], Ana Cecilia Millena[a], Lilya Matyunina[b], Mengnan Zhang[b], Jin Zou[a], Guangdi Wang[c], Qiang Zhang[c], Nathan Bowen[a], Vanessa Eaton[a], Gabrielle Webb[a], Shadyra Thompson[a], John McDonald[b], Shafiq Khan[a,*]

[a] Center for Cancer Research and Therapeutic Development, Clark Atlanta University, 223 James P. Brawley Dr. SW, Atlanta, GA, 30314, USA
[b] Integrated Cancer Research Center, School of Biological Sciences, Parker H. Petit Institute for Bioengineering and Bioscience, Georgia Institute of Technology, 315 Ferst Drive, Atlanta, GA, 30309, USA
[c] Department of Chemistry, RCMI Cancer Research Center, Xavier University, 1 Drexel Drive, New Orleans, LA, 70125, USA

ARTICLE INFO

*Keywords:*
JunD
c-MYC
Cell cycle regulation
Prostate cancer
Cancer initiation

ABSTRACT

JunD, a member of the AP-1 family, is essential for cell proliferation in prostate cancer (PCa) cells. We recently demonstrated that JunD knock-down (KD) in PCa cells results in cell cycle arrest in $G_1$-phase concomitant with a decrease in cyclin D1, Ki67, and c-MYC, but an increase in p21 levels. Furthermore, the over-expression of JunD significantly increased proliferation suggesting JunD regulation of genes required for cell cycle progression. Here, employing gene expression profiling, quantitative proteomics, and validation approaches, we demonstrate that JunD KD is associated with distinct gene and protein expression patterns. Comparative integrative analysis by Ingenuity Pathway Analysis (IPA) identified 1) cell cycle control/regulation as the top canonical pathway whose members exhibited a significant decrease in their expression following JunD KD including PRDX3, PEA15, KIF2C, and CDK2, and 2) JunD dependent genes are associated with cell proliferation, with MYC as the critical downstream regulator. Conversely, JunD over-expression induced the expression of the above genes including c-MYC. We conclude that JunD is a crucial regulator of cell cycle progression and inhibiting its target genes may be an effective approach to block prostate carcinogenesis.

## 1. Introduction

Prostate cancer (PCa) is the most prevalent malignancy in men worldwide and remains the frequent cause of cancer-related deaths in men [1–3]. Early stage PCa is localized in the prostate gland and is treatable by surgery and radiation therapy and the prognosis in these patients is very good. However, later stages of this disease metastasize to the bone and other tissues posing a significant problem for treatment [2,4–8]. The majority of PCa deaths are due to metastatic disease. Current treatments for metastatic disease are hormonal therapy and chemotherapy [4,6–8]. Hormonal therapies are based on the inhibition of biosynthesis and/or action of androgens; however, when cancer cells develop resistance to these treatments, they become castration resistant or hormone refractory prostate cancers [6–8]. There is no effective therapy for these cancers which are responsible for the mortality in majority of patients. Therefore, developing therapeutic strategies to target development and progression of metastatic prostate cancers will lead to significant increase in the survival of prostate cancer patients.

Despite recent breakthroughs in identifying specific PCa genes such as *ETS/ERG* gene fusions [3,9], *PTEN* deletions [3,10], *MYC* over-expression [11,12], *NKX3.1* loss of function [11,13], *AR*, *SPOP,* and *FOXA1* somatic mutations [3,8], the molecular mechanisms involved in the initiation and progression of PCa still remain to be clearly understood. The development of PCa occurs with uncontrolled cell proliferation which leads to the development of benign low-grade prostatic intraepithelial neoplasia (LGPIN), followed by high-grade PIN (HGPIN), a precursor for invasive carcinoma, which leads to the development of highly invasive intraductal carcinoma [14,15]. The initiation of carcinogenesis in the prostate is primarily dependent on deregulation of genes that control cell proliferation and as a result, causes either a loss of inhibitory controls of cell cycle progression or upregulation of factors which stimulate cell proliferation [16–18].

Transcription factors (TFs) have been implicated as important drivers of PCa, primarily due to their overexpression in PCa cell lines and PCa patient tissue samples. Well studied examples include c-MYC [11,12,19], ETS [9,20], GATA2 [21,22], and E2F3 [23,24]. Members of

* Corresponding author.
*E-mail address:* skhan@cau.edu (S. Khan).

https://doi.org/10.1016/j.canlet.2019.02.005
Received 4 August 2018; Received in revised form 4 February 2019; Accepted 5 February 2019

the activating protein-1 (AP-1) transcription factor family are often implicated as oncogenic cancer drivers [20,25–29]. The AP-1 transcription factor is composed of dimer combinations primarily formed between the Jun (JunB, c-Jun, and JunD) and Fos (FosB, c-Fos, Fra1, and Fra2) protein family members [29,30]. Jun proteins form homodimers (Jun–Jun) or heterodimers (Jun-Fos), while Fos proteins can only form heterodimers with Jun proteins that bind to the TPA-response element (TRE) or cyclic AMP-responsive elements (CRE) in the promoter regions of target genes [20,29,30]. AP-1 activity modulate through its dimer composition which leads to differential transcriptional and biological functions [20]. AP-1 regulates cellular proliferation, survival, apoptosis, inflammation, differentiation, locomotion, and plays a central role in oncogenesis [20,28,29]. The AP-1 transcription factors and their upstream kinases have been implicated in PCa initiation and progression [31–33]. For example, c-Jun or c-Fos overexpression increases cell proliferation and invasiveness of PCa cell lines [34]. Furthermore, high levels of these proteins are associated with PCa disease recurrence [33]. Previous studies also indicate that JunD along with Fra1 and Fra2 are essential in PCa proliferation and confer protection against radiation-induced cell death [35]. Our previous studies show that JunD is required for proliferation of PCa cells, while c-Jun and JunB had no effect on cell proliferation [29].

c-MYC, an oncogenic TF, is involved in regulating several biological activities including cell proliferation, apoptosis, and also carcinogenesis [36–40]. c- MYC protein is overexpressed in several cancers including PCa [11,36,37], but in normal (non-transformed) cells, c-MYC expression levels are low and its function is tightly regulated by developmental or mitogenic signals [40–42]. c-MYC regulates the cell cycle and cell metabolism. c-MYC levels accumulate as the initial response gene and are maintained at high levels throughout the cell cycle in the presence of growth factors [19,43]. In the presence of mutations, c-MYC levels become out of control thereby leading to tumorigenesis [19,40]. Several reports have described in-depth analyses of normal c-MYC function as well as its overexpression leading to carcinogenesis, but little is known regarding its regulation. We recently reported that in the absence of JunD protein in PCa cells, cell proliferation is inhibited along with a significant decrease in the levels of proteins involved in cell cycle regulation including c-MYC [29]. Furthermore, the over-expression of JunD significantly increased cell proliferation and colony formation in PCa cells [29]. This data suggested that JunD (as a part of AP-1 TF) regulates the expression of genes which are required for the progression of cell cycle and a decrease in JunD protein levels may result in decreased expression of these genes and inhibition of cell cycle.

In this current study, we investigated the changes in cell cycle regulatory genes following JunD knock-down (KD) in PCa cells by microarray and proteomic analysis. We identified down-regulated JunD dependent genes that are associated with cell cycle regulation. Our results demonstrated an essential role for JunD and JunD dependent genes in PCa initiation and carcinogenesis.

## 2. Materials and methods

### 2.1. Chemical and reagents

Antibodies against JunD (Cat. # sc-74), PRDX3 (Cat. # sc-59663), and c-MYC (Cat. # sc-40) were purchased from Santa Cruz Biotechnology, Inc. (Dallas, TX). Antibodies against CDK2 (Cat. # sc-2848), CDK4 (Cat. # sc-166373), KIF2C (Cat. # sc-81305), EIF1/B (Cat. # sc-390122), PEA15 (Cat. # sc-166678), Cyclin A or CCNA1 (Cat. # sc-271682), $\alpha_{2B}$-AR or ADRA2B (Cat. # sc-390430), PLCD4 (Cat. # sc-373875), TCF4 (Cat. # sc-166699), Annexin II or ANAX2 (Cat. # sc-28385), ELMO2 (Cat. # sc-365739), ERO1-Lα (Cat. # sc-100805), and Tropomyosin or PTMA (Cat. # sc-74480) were all provided as samples from Santa Cruz Biotechnology, Inc. (Dallas, TX). The antibody against Ki-67 (Cat. # NA59) was purchased from Calbiochem (Burlington, MA). The antibody against anti-α-Tubulin (Cat. #T5168) was purchased from Sigma-Aldrich (St. Louis, MO). Anti-mouse IgG-HRP was purchased from GE Healthcare (Piscataway, NJ). Goat anti-rabbit IgG-HRP (immunoglobulin horseradish peroxidase) and Rhodamine-phalloidin were purchased from Promega (Madison, WI). Small interfering RNA transfection reagent (Cat # sc-29528), JunD (Cat. # sc-3578), PRDX3 (Cat. # sc-40833), and Control-A (Cat. # 37007) siRNAs were all purchased from Santa Cruz Biotechnology, Inc. Lipofectamine 3000 Transfection Reagent and DAPI were purchased from ThermoFisher Scientific, Inc. (Waltham, MA). JQ1 inhibitor (Cat # 27400) was purchased from BPS Bioscience (San Diego, CA) and dissolved in dimethyl sulfoxide (Fisher Scientific) to a stock concentration of 10 mM, aliquoted and stored at −80 °C. G418 (Cat. # 345810) was purchased from Calbiochem.

### 2.2. Cell lines and cell culture

Human PCa cell lines (PC3 and DU145) were purchased from ATCC (Manassas, VA). Cells were cultured in the recommended growth media [MEM media supplemented with 5% fetal bovine serum (FBS)] in 100% humidity at 37 °C with 5% $CO_2$ as described previously [29]. DU145 cells overexpressing JunD (D1), generated from a previous study were cultured as above, with an addition of 200 ng/ml G418 [29].

### 2.3. Generation of JunD knock-out (KO) cells by CRISPR/Cas9 genome editing

PC3 JunD KO cells were generated using CRISR/Cas9 as previously described [44,45]. In brief, CRISPR/Cas9 single-guide RNAs (sgRNAs) targeting 2 locations on JunD exon 1 were identified using the CRISPR design tool provided by *Zhang's Lab* at MIT (http://crispr.mit.edu/) as follows, 5′-GCCTACCCCCCTGCGCGCCGA-3′ and 5′-GTTCGCGTAGAC AGGCGCTTC-3′ (Supplemental Fig. 1A). Each sgRNA was cloned into an all in one-WT Cas 9 plasmid vector, previously generated in Dr. Chunliang Li's Lab (St. Jude Children's Research Hospital, Memphis TN). Plasmids containing sgRNAs were validated by Sanger sequencing using the U6 promoter forward primer 5′-GAGGGCCTATTTCCCAT GAT-3′ and then transfected into PC3 cells using Lipofectamine 3000 reagent, according to the manufacture's protocol. Western blot analyses were performed to confirm the knock-out of JunD protein. JunD knock-out cells were used in additional functional assays.

### 2.4. Transient transfection with JunD, PRDX3, and control siRNAs

The transient knock-down of JunD or PRDX3 protein in PC3 and DU145 cells were performed using previously described methods [29]. In brief, PC3 and DU145 cells were transfected with 60 nM of JunD, PRDX3, or control siRNA using transfection reagents (Santa Cruz Biotechnology) following the manufacturer's recommendations. Seventy-two hours after transfection, the knock-down of JunD or PRDX3 expression in PC3 and DU145 were confirmed by Western blot analysis and then subjected to several functional analyses.

### 2.5. Cell proliferation assays

Cell growth assays were performed to examine the growth rates of PC3 wt and PC3 JunD knock-out (KO) cells generated by CRISPR/Cas9. Cells were seeded in 6-well plates at a density of $1 \times 10^5$ cells/well and cell proliferation was determined after 4 days. Cells were trypsinized and counted using a Cellometer as previously described [29,46]. To determine the growth rate, cells were also seeded in 24-well plates at a density of $2 \times 10^4$ cells/well and counted on days 1, 2, 4, 6, and 8 using a hemocytometer.

To determine the effects of the knockdown of JunD or PRDX3 on cell proliferation, DU145 and PC3 cells were seeded in 6-well plates at a density of $1.5 \times 10^5$ cells/well. Cell proliferation was examined 72 h following transient transfection with JunD or PRDX3, and control siRNAs. Cell growth assays were performed using cell counting in a

Cellometer.

### 2.6. Treatment of cells with JQ1 inhibitor

To determine dose-dependent effects of JQ1, DU145 cells were seeded in 24 well plates at a density of $2 \times 10^4$ cells/well (for cell proliferation assays) or at a density of $1.5 \times 10^5$ cell/well in 6 well plates (for protein lysates) overnight and then incubated with different concentrations of JQ1 (0, 0.1, 0.5, 1, 2.5, 5, and 10 μM) in the presence of 1% FBS for 72hrs. Control or JunD over-expressing DU145 cells (D1) were incubated in the presence or absence of 5 μM JQ1 for 72hrs using the same cell densities as mentioned above for cell proliferation assays or for protein lysates. Cells were counted using a hemocytometer and cell lysates were collected for western blot analyses.

### 2.7. Immunofluorescence of F-actin staining

Wild type and JunD knockout PC3 cells generated by CRISPR/Cas9 were grown ($0.5 \times 10^5$) on glass cover slips for 72 h, fixed and permeabilized as previously described [44]. Cells were stained with rhodamine-phalloidin for 30 min and DAPI for 10 min to detect F-actin filaments and the nuclei, respectively. Slides were mounted in Vectashield mounting medium (Vector Laboratories, Burlingame, CA) and images captured using Carl Zeiss 200M inverted microscope (Carl Zeiss, Thornwood, NY) at 20X magnification [29]. The cell areas were determined using Image J software.

### 2.8. Total RNA preparation

Total RNA from all human prostate cell lines used in this study was isolated using TRIzol (Life Technologies, Grand Island, NY) as previously described [29,46,47]. For quantitative real-time PCR (qRT-PCR), RNA concentrations and purity were determined using a Nanodrop 2000c Spectrophotometer (A260/280 ratio ≥ 1.9) as previously described [46]. For subsequent microarray studies, RNA samples (triplicate samples from each condition) were sent to Georgia Institute of Technology (Georgia-Tech, Atlanta, GA) for processing and analyses. The quality of the RNA was verified using an Agilent Bioanalyzer (Agilent Technologies) [48]. RNA samples with an RNA integrity number (RIN) of 10 were used for microarray analysis. The samples were diluted to a final concentration of 500 ng/μl and applied to an RNA chip according to the manufacturer's instructions [48,49].

### 2.9. Quantitative real-time PCR (qRT-PCR) analysis

The synthesis of cDNA from total RNA (2 μg) by reverse transcription was performed as previously described [50]. qRT-PCR was carried out in triplicate using GoTaq Master Mix (Promega, Madison, WI) on BioRad CFX Connect Real time PCR System (BioRad, Hercules, CA) as previously described [46]. Melting curves were generated to confirm the amplification of a single PCR product. Quantitation of the PCR results was based on the threshold cycle ($C_t$) and normalized to human GAPDH as previously described [46]. All human PCR primers were designed using Primer3 Plus software (https://primer3plus.com/cgi-bin/dev/primer3plus.cgi) and synthesized by Integrated DNA Technologies (Coralville, IA). All primers with their respective sequences are listed in Supplemental Table 1. Independent experiments were repeated at least three times for each sample/condition.

### 2.10. Microarray analysis

To investigate differential gene expression after JunD knockdown by siRNA in PC3 cells, microarray analyses were conducted on the GeneChip® Human Genome U133 Plus 2.0 Arrays (Affymetrix), providing a comprehensive analysis of genome-wide expression on a single array. Gene expression signals from each array were processed to Affymetrix.CEL files using the Affymetrix Expression Console (EC) Software Version 1.4 using the Robust Multi-Array Average (RMA) normalization method [48,51]. Raw data was normalized using SST-RMA algorithm. The normalized expression values from all samples (N = 2, in triplicates) were log2 transformed. Differentially expressed genes were identified as fold changes (FC) > 1.1 (up or down) and p-value < 0.05 using Student t-test. Genes were annotated using Ingenuity Pathway software (http://www.ingenuity.com/) for cellular functions during differentiation and interactions and were mapped according to their instructions [52].

### 2.11. Western blot analysis

Following siRNA transient transfections, PC3 and DU145 cell lysates from several independent experiments were collected as previously described [29]. In brief, equal amounts of proteins (50 μg) were separated by electrophoresis using 10% SDS-polyacrylamide gels and then transferred to PVDF membranes (Millipore, Billerica, MA). After being blocked with 5% milk, the membranes were incubated with specific primary antibodies (1:800 dilution for JunD; 1:500 dilution for anti-PRDX3, anti-CDK2, anti-CDK4, anti-KIF2C, anti-EIF1, anti-PEA15, anti-CCNA1, anti-ADRA2B, anti-TCF4, anti-ANAX2, anti-ELMO2, and anti-ERO1-Lα; 1:200 dilution for anti-PLCD4, anti-c-MYC, and anti-PTMA; 1:3000 dilution for anti-α-Tubulin) overnight at 4 °C and then incubated with appropriate horseradish peroxidase-conjugated secondary antibody for 1 h. The blots were developed using Millipore Luminata Forte (EMD Millipore, Billerica, MA) and visualized by Syngene PXI 6 imagining system (Syngene, Frederick, MD). All blots were probed for α-Tubulin as loading controls. The relative intensities of specific protein bands were determined by ImageJ software (NIH version: 1.8.0_112).

### 2.12. Proteomics

#### 2.12.1. Cell lysis and protein extraction

PC3 cells were subjected to proteomic analysis as previously described, with minor modifications [53,54]. In brief, PC3 cells were plated at a total density of $1 \times 10^6$ cells in 6-well plates per condition and transfected the next day with control or JunD siRNA for 72 h. Biological replicates were prepared using the same conditions. Following siRNA transfections, the cell pellets from PC3 control and PC3-JunD KD cells were lysed with 1 ml M-Per Mammalian Protein Extraction Reagent (Thermo Scientific) containing 10 μl phosphatase inhibitors and 10 μl protease inhibitors (Thermo Scientific) according to manufacturer's instructions. The samples were sonicated followed by centrifugation at 16,000 × *g* for 5min. The supernatant of each sample was collected, and the protein concentrations were determined by the BCA protein assay (Pierce Biotechnology, Rockford, IL) following manufacturer instructions. Samples were subjected to reduction, alkylation, and trypsin digestion as previously described [53,54]. The trypsin-digested samples were used in the next procedure.

#### 2.12.2. Isobaric labeling with tandem mass tag (TMT).

Tandem mass tags ($TMT^6$) (Thermo Scientific) with increasing molecular weights ranging from 126 to 131 Da were applied as isobaric tags to determine differential protein levels between PC3 control cells and PC3 JunD knockdown cells as previously described [53,54]. The labeled peptide mixtures were combined at equal ratios and purified by a strong cation exchange (SCX) column.

#### 2.12.3. Fractionation of labeled peptide mixture by using a strong cation exchange column

The combined TMT-labeled peptide mixtures were fractionated with a SCX column (Thermo Scientific) on a Shimadzu Ultra-Fast Liquid Chromatography (UFLC) equipped with an ultraviolet detector (Shimadzu, Columbia, MD), and a mobile phase consisting of buffer A (5 mM $KH2PO_4$, 25% acetonitrile, and pH 2.8) and buffer B (buffer A

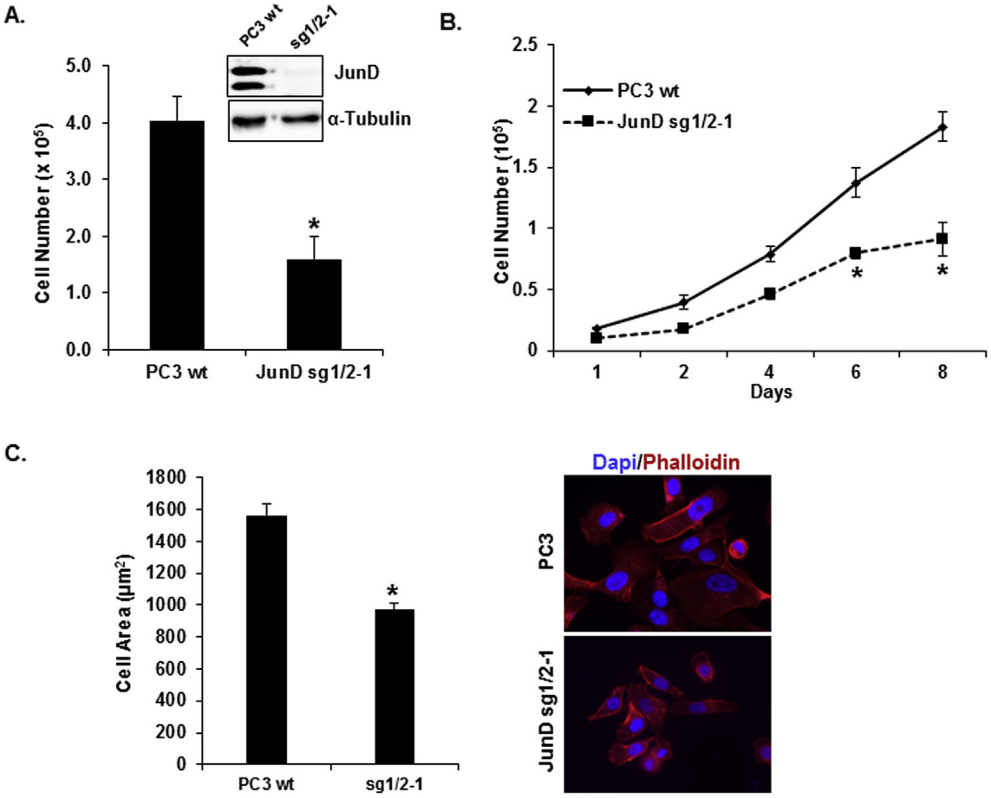


**Fig. 1. Generation of PC3 JunD Knockout (KO) cells by CRISPR/Cas9 genome editing.** JunD KO in PC3 cells was confirmed by Western blot analysis (insert). Cell proliferation assays were performed to measure ***(A)*** cell growth (4 days) and ***(B)*** growth curve (1–8 days) of PC3-JunD KO cells (JunD sg1/2-1) and compared with PC3 WT (control cells). **C.** Cell size was determined by Image J *(left panel)* and visualized by staining cells with DAPI (nuclei) and Phalloidin (actin filaments), *right panel*. The statistical analyses were performed by one-way ANOVA analyses and Tukey Multiple Comparison test. Each bar represents Mean ± SEM (n = 3) $^{*}p < 0.001$.

plus 350 mM KCl), as previously described [53,54]. In total, sixty fractions were collected, lyophilized, and combined into 14 final fractions based on SCX chromatogram peaks. The collected fractions were desalted using a $C_{18}$ solid-phase extraction (SPE) column (Hyper-Sep SPE Columns, Thermo Scientific) as previously described [53,54]. Briefly, the 14 combined fractions were each adjusted to a final volume of 1 ml containing 0.25% trifluoroacetic acid (TFA) solution. The eluted samples were lyophilized prior to the liquid chromatography mass spectrometry (LC-MS/MS) analysis.

#### 2.12.4. LC-MS/MS analysis on LTQ-Orbitrap

Peptides were analyzed on an LTQ Orbitrap.XL (Thermo Scientific, Waltham, MA) instrument interfaced with an Ultimate 3000 Dionex LC system (Dionex, Sunnyvale, CA). High mass resolution was used for peptide identification and high energy collision dissociation (HCD) was employed for reporter ion quantification as previously described [53,54].

#### 2.12.5. Database search and TMT quantification

The protein search algorithm SEQUEST was used to identify and quantify unique peptides using the Proteome Discoverer data processing software (version 1.2, Thermo Fisher Scientific, Waltham, MA). Peptides reported by the search engine were accepted only if they met the false discovery rate of $P < 0.05$ (target-decoy database). The ratios of TMT reporter ion abundances in MS/MS spectra generated by HCD from raw data sets were used for TMT quantification. Fold changes in proteins between PC3 control and PC3-JunD KD samples were calculated as previously described [53,54].

### 2.13. Ingenuity Pathway Analysis (IPA)

Our datasets generated from microarray and proteomic mass spectrometric analyses were analyzed using Ingenuity Pathway Analysis (IPA) software (Ingenuity Systems, Inc., Redwood City, CA; http://www.ingenuity.com) [52]. Ingenuity Knowledge Based tool was used to identify all significant biological functions and canonical pathways that involve differentially expressed genes (DEGs) and differentially regulated proteins (DEPs). The IPA program applies Fisher's exact test to calculate a p-value that represents the probability of the DEGs and DEPs in the pathway being found together due to random chance. Specifically, genes and proteins identified in the microarray and proteomics, respectively, with differential expression p-values < 0.05 and fold-changes ≥ 1.5 were used as focus genes/proteins. Pathways with *p*-values < 0.05 were considered significantly enriched.

### 2.14. Analysis of JunD and JunD dependent genes in prostate cancer patient tissues from The Cancer Genome Atlas (TCGA)

The expression matrix of *JunD* in prostate tissues was obtained from the gene expression of RNAseq (Illumina HiSeq) dataset for prostate adenocarcinoma (PRAD) using the TCGA database. The raw data of gene expression levels were log2(x+1) transformed and processed at the UCSC Xena repository as previously described [55]. Reprocessed data were downloaded using UCSC Xena Functional Genomics Explorer (https://xenabrowser.net/). Samples with no data recorded (null data) were excluded from plots in data analysis. Boxplots were generated using Sigma Plot® software.

### 2.15. Statistical analysis

All data are presented as the mean ± SEM. The types of statistical tests that were used to evaluate statistical significance are indicated in the text and/or figure legends. $P < 0.05$ indicates statistical significance. All statistical analyses were performed using Sigma Plot® software, unless otherwise specified.

## 3. Results

### 3.1. JunD KO attenuates cell proliferation of prostate cancer cells

In our previous study, we showed that JunD plays an essential role in cell proliferation of prostate cancer cells [29]. To confirm JunD's role in cell proliferation, we generated JunD knock out (KO) prostate cancer cells (PC3-JunD KO) using CRISPR/Cas9 genomic editing (Fig. 1, Supplemental Fig. 1). We detected a complete knockout of JunD protein in Clone sg1/2-1 (Fig. 1A and Supplemental Fig. 1B). In the absence of JunD protein, cell proliferation was significantly reduced (61%, $p < 0.001$) compared to PC3 WT cells (Fig. 1A, Supplemental Fig. 1C) with a significant decrease in proliferation in a time-dependent manner (Fig. 1B) and a decrease in cell size (Fig. 1C, Supplemental Fig. 1D). Because JunD KO cells' growth rate slowed down tremendously causing difficulty in carrying out additional functional studies, we utilized cells with transient JunD knock-down throughout the remainder of this study.

### 3.2. JunD knockdown decreases expression of cell cycle-related genes including MYC

We previously demonstrated that JunD knock-down (KD) in PCa cells results in cell cycle arrest in $G_1$-phase concomitant with a decrease in several proteins involved in cell proliferation and cell cycle regulation (cyclin D1, Ki67, c-MYC, and Id1), but an increase in p21 protein [29]. Furthermore, the over-expression of JunD significantly increased cell proliferation in these cells suggesting that JunD regulates the expression of genes which are required for the progression of the cell cycle [29]. To test this possibility and to elucidate the key molecules and signaling pathways in JunD-mediated cell proliferation of PCa cells, PC3 cells treated with JunD siRNA or control siRNA were subjected to microarray and proteomic analyses as illustrated in Fig. 2. We confirmed an 85% knock-down of JunD protein in comparison with cells transfected with control siRNA as determined by Western blot analysis (Fig. 2). Following microarray and proteomic analysis, we identified differentially expressed genes (DEGs) and proteins (DEPs) that were down-regulated or up-regulated in PC3 JunD KD cells compared to siControl PC3 cells. From microarray analysis, a total of 54,675 molecules were quantified, and among these, 3,103 were found to have a differential expression ($p < 0.05$), including 1,598 upregulated and 1,505 downregulated molecules (Table in Fig. 2). From the proteomic analysis, a total of 5,605 protein molecules were quantified, and among these, 2,056 were found to have a differential expression ($p < 0.05$), including 1,007 upregulated and 1,049 downregulated protein molecules (Table in Fig. 2).

We detected a signature by recruiting several probes with a cutoff value of > 2.0-fold change in JunD-deficient PC3 cells compared with control cells as depicted in the Venn diagram (Fig. 3A). Hierarchical clustering analysis was used to compare differential ($p < 0.01$) JunD dependent gene expression between PC3 control and PC3-JunD KD cells as shown in Fig. 3B. The top 20 up- or down-regulated genes are shown in Supplemental Table 2. Because our previous studies suggested that the absence of JunD leads to cell cycle arrest and the down-regulation of several cell-cycle associated proteins [29], we focused primarily on the array of genes that were down-regulated as a result of JunD KD in the present study. The top 10 down-regulated genes from microarray data are shown in a heat map visualization and include JunD, PRDX3, EPHA5, CCNA1, NAGA, ADRB2, F2RL2, CBX4, STX6, and NDUFAF4 (Fig. 3C).

To identify altered pathways and to explore the potential function (s) of down-regulated mRNAs in JunD-deficient cells compared to control cells, Ingenuity Pathway Analysis (IPA) was used to identify the biological processes, molecular and cellular functions, and their possible involvement in diseases and disorders. The pathways and functions were determined by an enrichment score ($p < 0.05$) as previously

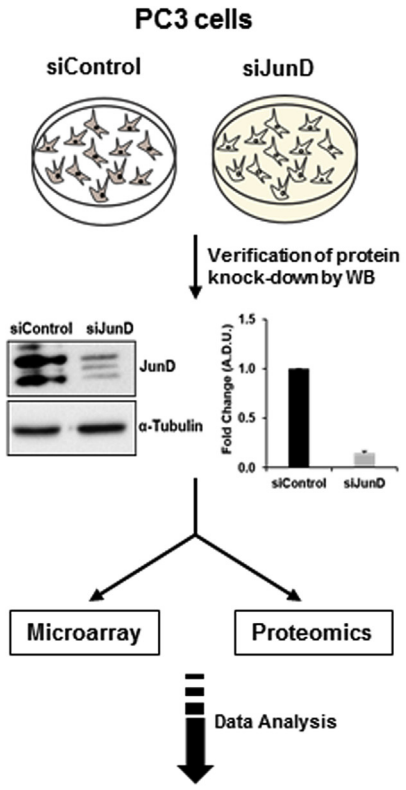


| | # Molecules | D.E. $p < 0.05$ | Down-regulated $p < 0.05$ | Up-regulated $p < 0.05$ |
|---|---|---|---|---|
| Microarray | 54,675 | 3,103 | 1,505 | 1,598 |
| Proteomics | 5,605 | 2,056 | 1,049 | 1,007 |

**Fig. 2. Schematic diagram showing procedures used to examine differential gene expression and protein levels following JunD knock-down in PC3 cells.** Following JunD knock-down by siRNA and verification by western blot analysis, PC3-JunD knockdown and siControl lysates were subjected to Microarray and Proteomic analysis. Differentially expressed molecules were selected based on fold change increase or decrease in their expression ($p < 0.05$).

described [52]. JunD deficiency was associated with several changes in specific signaling pathways. Cell cycle control/regulation was predicted to be one of the top pathways whose members exhibited decreased gene expression following JunD knock-down (Fig. 3D). Similar to transcriptome analysis, most significant differences in protein expression levels ($p < 0.05$) were also observed in proteins involved in cell cycle regulation (top 20 DEPs up or down ($p < 0.05$), Supplemental Table 3) according to IPA. Furthermore, in an upstream pathway analysis using proteomics data, MYC, a key regulator of cell cycle control, was one of the top upstream regulators (Fig. 3E, left) in which its activity was dramatically inhibited following JunD depletion (Fig. 3E, right). IPA analysis of proteomics data focusing on MYC and its relationship with target molecules indicates that the inhibition of MYC leads to the downregulation of several cell cycle associated proteins including CDKs, PRDX3, ACTN4, and FASN (green color) (Fig. 3F).

### 3.3. Integrated analysis of transcriptome and proteome in PC3-JunD knockdown cells

To further determine the molecular signature associated with JunD-mediated cell proliferation/cell cycle regulation, we performed a comparative analysis of genomic and proteomic data using IPA (using only significantly down-regulated molecules, $p < 0.05$). We

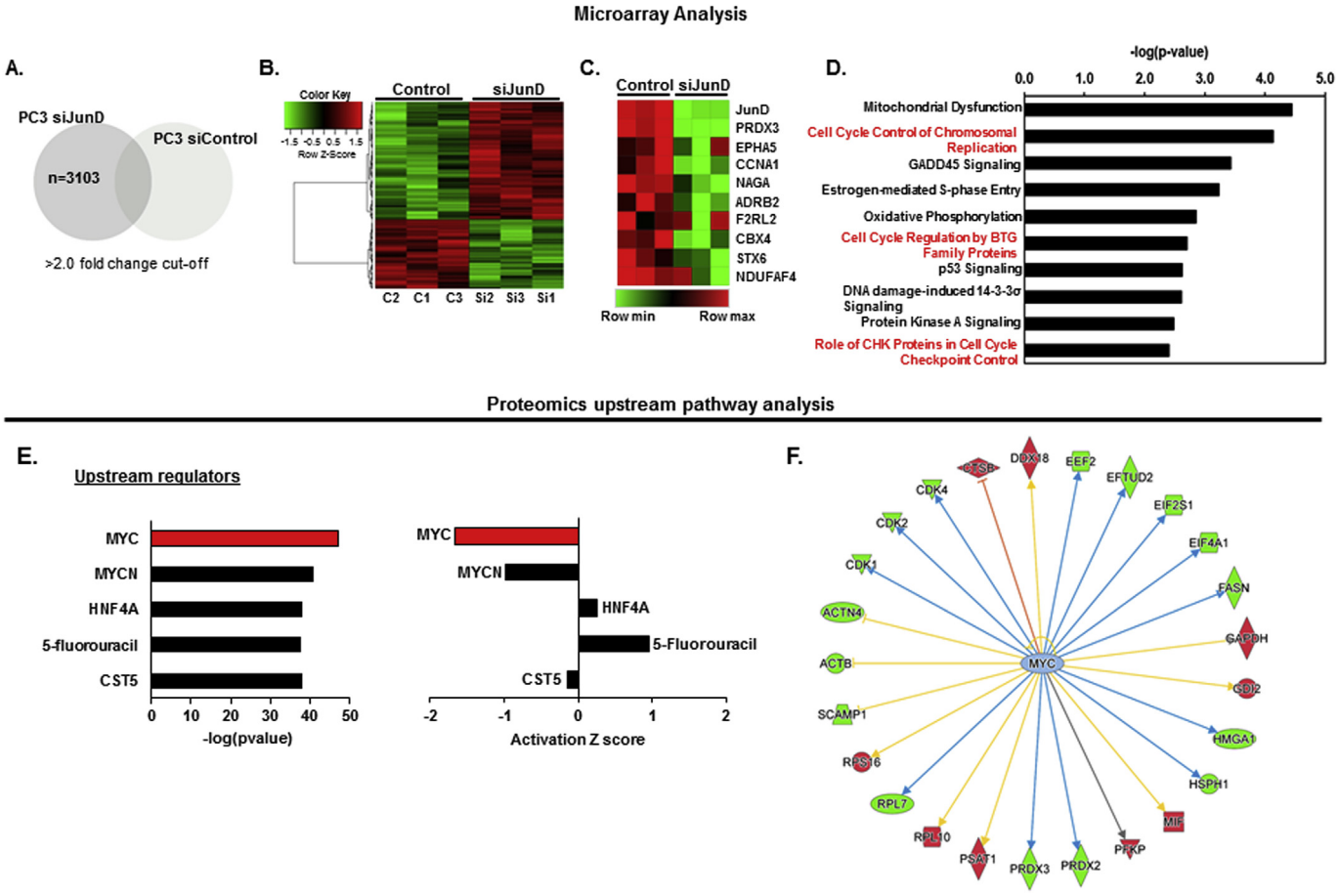


**Fig. 3. Overview of microarray and proteomic pathway analyses from PC3 cells ± JunD.** ***A.*** Putative probes regulated by JunD were identified from genes upregulated/downregulated at least 2-fold in PC3 cells after JunD knockdown compared with siControl cells. $P < 0.05$ was considered as significant enrichment. ***B.*** Heatmap of differentially expressed genes (F.C = 1.1, $p < 0.01$). ***C.*** A RNA microarray analysis showing the top 10 downregulated genes in PC3-JunD deficient cells which are also involved in cell cycle regulation. ***D.*** Cell Cycle Control/Regulation was one of the top pathways whose members exhibited gene expression down-regulation after JunD knock-down in PC3 cells, according to Ingenuity Pathway Analysis (IPA). Pathways with *p*-values < 0.05 were considered significantly enriched. ***E, F.*** IPA upstream pathway analysis of mass spectrometry proteomic data revealed that MYC, a known master regulator of cell cycle, is one the top upstream regulator of JunD targets. *Green and red color in ***F*** indicates a downregulation or upregulation of protein levels, respectively, as a result of MYC inhibition. (For interpretation of the references to color in this figure legend, the reader is referred to the Web version of this article.)

investigated the functional annotation and interrelation of 3 groups: unique genes found only in microarray data, unique proteins found only in proteomic data, and genes/proteins shared between both microarray and proteomic data. The overlap between protein and mRNA analyses are depicted in Fig. 4A. The top 10 down-regulated molecules for each category are listed below its respective group. This data analysis revealed that 92% of genes (out of 1,524 genes) and 88% of proteins (out of 1,028 proteins) were unique to microarray or proteomic data, respectively, in JunD-deficient cells, which are 1408 DEGs and 913 DEPs that were down-regulated. Additionally, 45% genes/proteins (115 molecules) were shared between the two groups. Using canonical pathway analysis, these molecules were categorized to related biological pathways. Among other significantly altered signaling pathways, cell cycle control of chromosomal replication was identified as one of the top significantly enriched canonical pathways of the genes/proteins altered in JunD deficient cells (Fisher' exact test, $P < 10^{-3}$, Table 1, Top Canonical Pathways section). 75 of these molecules were identified as involved in cell cycle regulation (top 10 listed in Fig. 4A, full list provided in Supplemental Table 4). IPA analysis also predicted that the majority of these molecules are associated with the MYC pathway, which indicates their possible role in cancer progression in addition to their involvement in cell cycle regulation (Fig. 4B). Furthermore, the annotation of these molecules indicates cancer among other diseases as the top 5 most associated disease and function based on the ranking of $-\log_{10}$P (Table 1, Top Diseases section). These analyses also highlighted JunD dependent molecules that participated in major molecular functions including RNA Post-Transcriptional Modification (63%, *p*-value = 2.10E-04 - 3.8E-11), Cell Death and Survival (59%, *p*-value = 7.01E-03 - 4.77E-10), Cell Cycle 41%, *p*-value = 7.01E-03 - 6.80E-09), Protein Synthesis (24%, *p*-value = 8.29E-04 - 1.72E-07), and Cellular Assembly and Organization (45%, *p*-value = 7.01E-03 – 2.35E-07), as shown in Supplemental Table 5.

### *3.4. Validation of JunD dependent genes and proteins identified by microarray and proteomics*

Among the 75 down-regulated genes/proteins identified to play a role in cell cycle regulation, we initially focused on 6 genes/proteins (PRDX3, CDK2, CDK4, EIF1, KIF2C, and PEA15) which were significantly down-regulated in PC3-JunD KD cells compared to PC3 control cells. Validation of microarray data was carried out using qRT-PCR on the same RNA samples used for transcriptome microarray analysis. Western blot analyses were performed to detect and validate the expression levels of these proteins. Additional independent experimental samples were also collected for both RNA and protein for biological replicates. We also confirmed the selected gene/protein expression levels in DU145 cells after the knock-down of endogenous JunD. As shown in Fig. 5, the expression patterns of the six selected

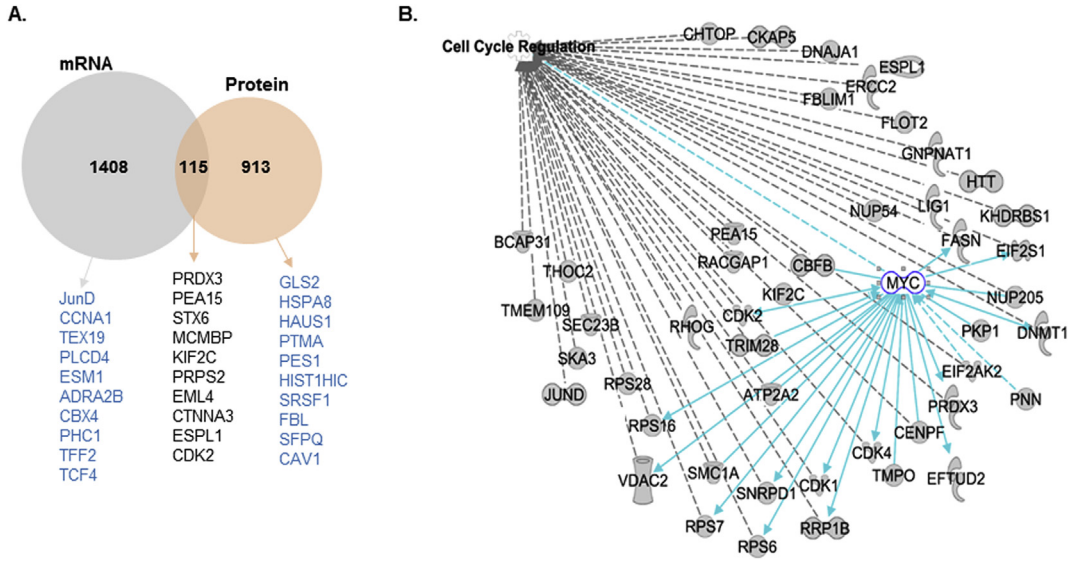


**Fig. 4. Integrating genomics and proteomic analyses by Ingenuity Pathway analysis. *A.*** Venn Diagram representing pair-wise comparison of microarray and proteomics molecules that were significantly downregulated ($p < 0.05$). The overlap represents the common molecules (115) identified by both microarray and proteomic analyses, and 75 of those genes being cell cycle-related. The top 10 down-regulated molecules for each category are listed below its respective group. ***B.*** JunD targets are involved in cell cycle regulation and are associated with MYC pathway, according to IPA.

**Table 1**
Summary of ingenuity pathway analysis.

| Pathway Analysis | P-value |
|---|---|
| **Top Canonical Pathways** | |
| EIF2 Signaling | 5.30E-09 |
| Regulation of eiF4 and p70S6K Signaling | 1.32E-06 |
| Cell Cycle Control of Chromosomal Replication | 1.55E-06 |
| **Top Upstream Regulators** | |
| MYC | 1.13E-10 |
| E2F1 | 1.71E-09 |
| sirolimus | 1.76E-06 |
| **Top Molecular and Cellular Functions** | |
| RNA Post-Transcriptional Modification | 2.10E-04 – 3.84E-11 |
| Cell Death and Survival | 7.01E-03 – 4.77E-10 |
| Cell Cycle | 7.01E-03 – 6.80E-9 |
| Protein Synthesis | 8.29E-04 – 1.72E-07 |
| **Top Diseases** | |
| Cancer | 7.01E-03 – 2.31E-08 |
| Organismal Injury and Abnormalities | 7.01E-03 – 2.31E-08 |
| Tumor Morphology | 6.35E-03 – 2.31E-08 |
| **Top Networks** | |
| Cell Morphology, Cellular Function and Maintenance | |
| Cell Cycle, Cell Death and Survival, Cellular Assembly and Organization | |
| Protein Synthesis, RNA Post-Transcriptional Modification | |

The includes shared analysis between Microarray and Proteomics ± JUND of down-regulated ($p < 0.05$) molecules.

significantly down-regulated gene/proteins in qRT-PCR (Fig. 5A and B) and Western blot analysis (Fig. 5C) were consistent with the microarray and proteomic analysis ($P \leq 0.05$), which demonstrated the reliability of the microarray and proteomic data. Among the six validated genes/proteins, the most significantly down-regulated gene/protein was PRDX3 ($p < 0.01$) in both PC3 and DU145 JunD-deficient cells. JunD mRNA and protein levels were also determined by qPCR and western blot analysis which confirmed a significant decrease of JunD protein in PC3 (62% decrease, $p < 0.05$) and DU145 cells (52% decrease, $p < 0.05$) in comparison with the cells transfected with the control siRNA. The relative protein levels of the selected genes normalized with α-Tubulin levels are indicated adjacent to the Western blot image (Fig. 5D). These results confirmed that the selected genes are indeed JunD dependent genes. We also confirmed gene expression and protein levels of molecules that exhibited a significant decrease in mRNA levels, but not protein levels (Supplemental Fig. 2) and also molecules which exhibited a significant reduction in protein levels, but not in mRNA levels (Supplemental Fig. 3).

### 3.5. JunD effects on cell proliferation are mediated via c-MYC signaling

On the basis of the findings that JunD-deficient cells exhibited a decrease in the expression of JunD dependent genes that are involved in cell cycle regulation, we further examined the role of JunD with respect to their protein levels in DU145 cells over-expressing JunD. We first confirmed the over-expression of JunD protein and the increase in proliferation of JunD over-expressing cell line (D1) compared to the control (vector) cells (Fig. 6) [29]. As shown in Fig. 6A, D1 cells exhibited a 2-fold increase ± 0.27 ($p < 0.05$) in cell numbers compared to the control cells. Increased proliferation correlated with the increase in JunD protein levels (insert). D1 cells also displayed a significant increase in c-MYC, PRDX3, KIF2C, and CDK2 protein levels compared to the control cells (Fig. 6B). To further demonstrate that JunD-induced proliferation requires MYC signaling, PCa cells were treated with JQ1, a known inhibitor that targets c-MYC protein and suppresses cellular growth [56,57]. The dose-dependent effects of JQ1 on cell proliferation in DU145 cells were established using different doses ranging from 0.1 to 10 μM. JQ1 significantly inhibited cell proliferation and induced a reduction in the levels of c-MYC protein in a dose-dependent manner (Supplemental Fig. 4A). Maximum inhibition was observed at 5 μM (Supplemental Fig. 4B). Control and JunD overexpressing (D1) cells were then treated with 5 μM JQ1 which resulted in a significant inhibition in cell proliferation ($p < 0.001$) (Fig. 6C) and a decrease in c-MYC and JunD dependent genes (Fig. 6D). There was also a significant decrease in Ki-67 protein level, a marker for cell proliferation, in both control and JunD overexpressing cells.

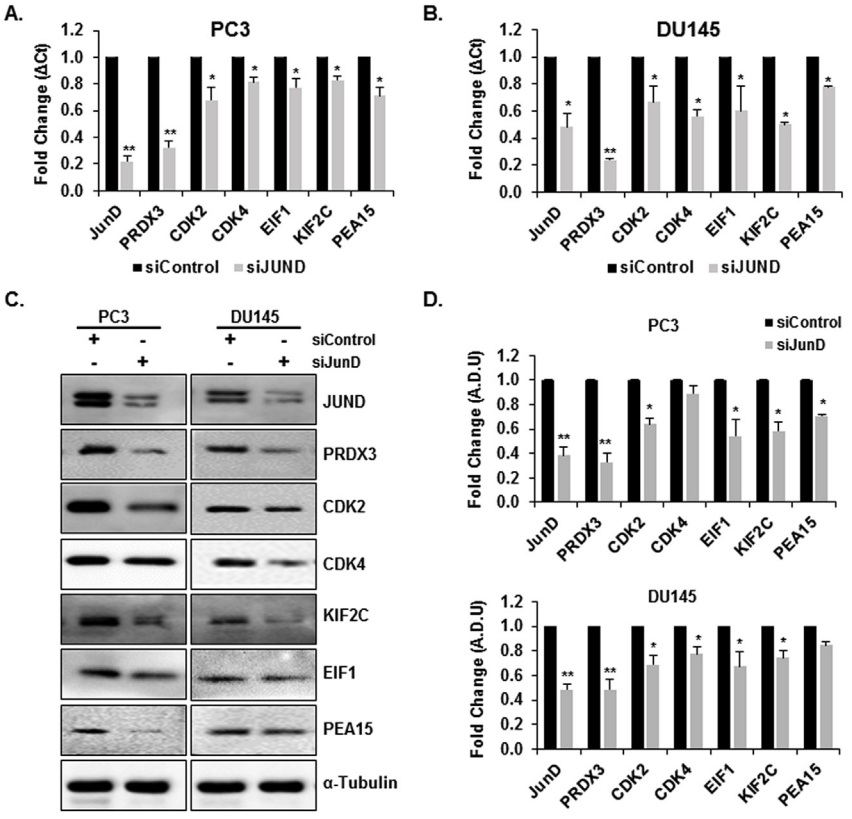


**Fig. 5. Validation of the expression of the integrated genes and proteins identified.** Validation of the Microarray results of selected genes from JunD knockdown by qPCR analysis of JunD, PRDX3, CDK2, CDK4, EIF1, KIF2C, and PEA15 gene expression after JunD knockdown in ***A.*** PC3 and ***B.*** DU145 cells. ***C.*** Protein levels determined by Western blot analysis ***D.*** Quantitative analysis of relative protein levels. Normalization was performed relative to the signal obtain with α-Tuburalin. Each bar represents Mean ± SEM (n = 3). Asterisks represent significantly different from control groups (**$p < 0.01$, *$p < 0.05$). Statistical significance was determined by One Way ANOVA and Duncan's Pairwise Multiple Comparison Method.

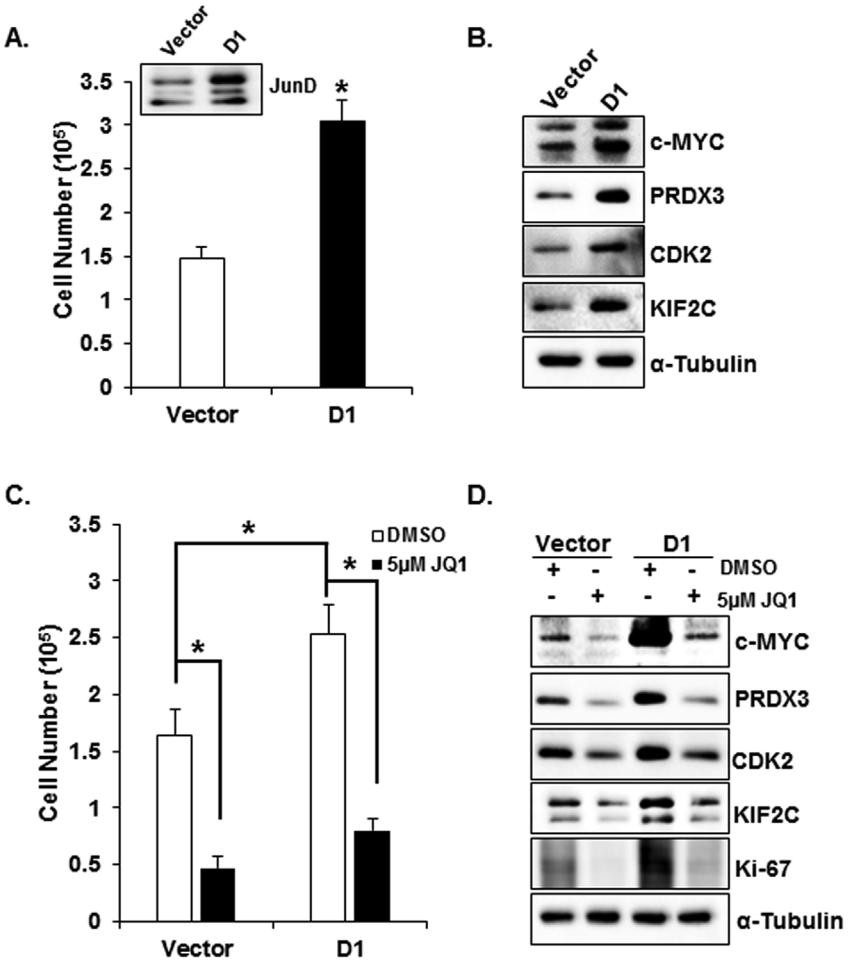


**Fig. 6. JQ1, a c-MYC inhibitor, suppresses JunD-mediated cell proliferation and JunD dependent genes' protein levels.** ***A.*** DU145 cells overexpressing JunD (D1) and DU145 cells containing an empty vector (V6), pcDNA3.1 were plated and allowed to grow for 72 h, followed by cell counting. Statistical significance was determined using Student's *t*-Test ($p < 0.001$). ***B.*** Western blot analyses confirming JunD overexpression in D1 cells (insert) and the protein levels of JunD dependent genes. α-Tubulin was used as a loading control. ***C.*** Cells treated with JQ1 (5 μM) were subjected to cell proliferation assays, and ***D.*** western blot analysis for JunD dependent genes. Statistical significance (*$p < 0.001$) for ***(C)*** was determined by one-way ANOVA and Duncan's Pairwise Multiple Comparison Method.

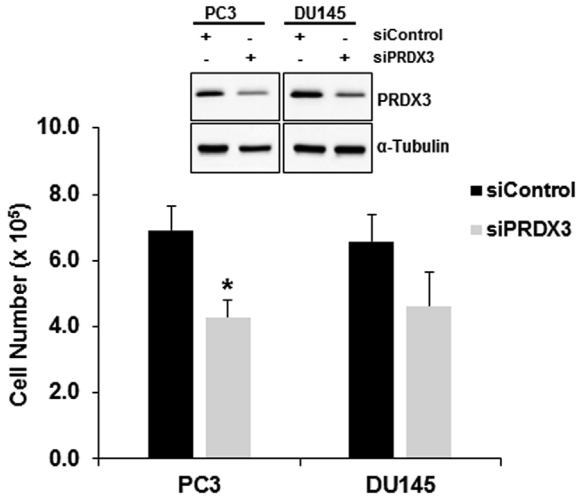


**Fig. 7. PRDX3 is required for cell proliferation of PC3 and DU145 cells.** PC3 and DU145 cells were transfected with either control or PRDX3 siRNA to knock-down the expression of PRDX3. Bar graph shows cell proliferation after transfections with control (siControl) or PRDX3 siRNA. Each bar represents Mean ± SEM (n = 3). *The Student t-test was used to determine the significant difference from respective control groups ($p < 0.05$). Levels of PRDX3 after transfection with siControl and PRDX3 siRNA were determined by western blot analysis (insert).

### 3.6. PRDX3 knock-down inhibits cell proliferation in PCa cells

To confirm requirement of JunD dependent genes for PCa cell proliferation, we examined PRDX3, the top hit that was down-regulated by JunD KD in PC3 cells in both groups. PRDX3 is also a key player in cell proliferation and is involved in promoting cell survival in PCa [58]. PRDX3 KD by siRNA in PC3 and DU145 cells was confirmed by western blot analysis, while the control siRNA had no effect on its protein levels (insert, Fig. 7). PRDX3 protein levels were significantly reduced (50% decrease, $p < 0.05$) in comparison to the controls in both PC3 and DU145 cells. The relative protein levels of PRDX3 were normalized to α-Tubulin (quantitative data not shown). The proliferation of PC3-PRDX3 and DU145-PRDX3 KD cells were also examined by cell counting 72 h after siRNA treatment. Our data indicate that the knockdown of PRDX3 resulted in a significant reduction in cell proliferation in PC3 (36% inhibition, $p < 0.05$) and DU145 (42% inhibition, $p < 0.05$) cells (Fig. 7). These results suggest that JunD dependent gene, PRDX3, is required for cell proliferation of PCa cells.

### 3.7. JunD expression analysis in prostate tissues from TCGA

We explored the expression profile of *JunD* mRNA in prostate tissues using The Cancer Genome Atlas (TCGA) dataset. There were a total of 623 samples, including 504 prostate primary tumor tissues, 118 normal prostate tissues, and one metastatic tissue. Overall, there was no significant difference in *JunD* levels in normal and primary prostate tumor tissues (Fig. 8A). We further examined *JunD* levels only within the primary tumor samples. The results showed that 71 primary tumor tissues had significantly higher *JunD* mRNA levels compared to the rest of the samples (Fig. 8B). Out of these 71 primary tumor samples with high *JunD*, 21% showed higher expression of c-MYC, 45% of *PRDX3*, 55% of *CDK2*, 17% of *KIF2C*, 44% of *PEA15*, and 52% of *EIF1*, as shown in Fig. 8C.

## 4. Discussion

It is well established that prostate carcinogenesis results from the uncontrollable growth of cells in the prostate gland due to various factors (inflammation, oxidative stress, DNA damage, cytokines, and certain mutations) that alter the normal gene regulation of a cell and its cell cycle. However, the precise molecular mechanisms involved in PCa initiation and progression are persistently being elucidated. In our previous study, we demonstrated the essential role of JunD in PCa cell proliferation and its regulation of several genes required for the progression of the cell cycle [29]. Findings from this study suggested that a decrease in JunD protein may result in decreased expression of cell cycle associated genes thereby leading to the inhibition of cell cycle [29]. In the present study, we confirmed the role of JunD in PCa cell proliferation by generating JunD knockout cells using CRISPR/Cas9 genomic editing. We also attempted to identify JunD regulated genes which are involved in cell cycle regulation by the analyses of the genome and proteome of JunD deficient cells. Here, we show a relationship at the molecular level between these two components, JunD and JunD-dependent genes, which establishes the mechanism(s) of JunD-driven cell proliferation in PCa cells.

To explore the involvement of JunD and its regulation of genes involved in cell proliferation and cell cycle regulation in prostate cancer, we analyzed the levels of deregulated mRNAs and proteins in JunD deficient cells using microarray and proteomics data, respectively, and then compared the biological functional processes and regulators identified in both data sets. Using a knowledge-based pathway analysis (IPA), we identified common features in both transcriptomic and proteomic data including the down-regulation of PRDX3, CDKs, and others. Several biological processes including cell cycle control/regulation, cell survival, cell morphology, and cellular motility were found in both transcriptomic and proteomic analysis to be altered in JunD deficient cells. The deregulation of these biological processes has been previously linked to carcinogenesis [16–18].

While in both datasets, over one thousand genes and proteins exhibited a downregulation of expression levels due to JunD KD, they did not show the same level of deregulation. The levels of deregulated mRNAs were not an accurate reflection of deregulated proteins. In simpler terms, genes that exhibited a significant decrease at the mRNA levels did not necessarily show a significant reduction at the protein level, and vice versa. These differences were predominately observed at the protein level with little to no corresponding changes at the mRNA level. c-MYC, in particular, was down-regulated at the protein level in PC3 JunD deficient cells, but not its mRNA levels, suggesting post transcriptional regulation of c-MYC by JunD. This type of phenomenon has been previously described in several studies indicating a poor correlation between mRNA expression and protein abundance; and could be due to various factors including RNA binding proteins and/or miRNAs that regulate specific genes by post-transcriptional and/or post-translational modifications [51,59–61]. The low correlation found in this study, corroborate with a previous study suggesting that protein levels correlated with only 20–40% of corresponding mRNA levels [61,62]. Of the shared genes and proteins significantly down-regulated ($p \leq 0.05$) in JunD-deficient cells, 65% are involved in cell cycle control/regulation and their expressions are dependent on the presence of JunD (JunD-dependent genes). Interestingly, c-MYC, a known master regulator of the cell cycle and critical player in carcinogenesis was found to be an upstream regulator of deregulated JunD-dependent genes in which its activity is significantly inhibited in JunD deficient cells. Furthermore, inhibition of c-MYC is predicted to lead to the inhibition of several JunD dependent genes (Fig. 3F). Our data suggests an interplay between JunD and c-MYC transcriptional regulation of genes leading to PCa development and progression.

Several transcription factors (TFs) have been reported to regulate cell proliferation. TFs play an essential role in determining the fate of a cell by affecting the expression of target genes involved in cell proliferation, differentiation, and programmed cell death [63]. Under certain conditions, some of these factors are capable of deregulating expression of genes involved in the cell cycle control and/or in programmed cell death resulting in uncontrolled proliferation of the cell, thereby leading to carcinogenesis [63]. AP-1 TFs, consisting of JUN and

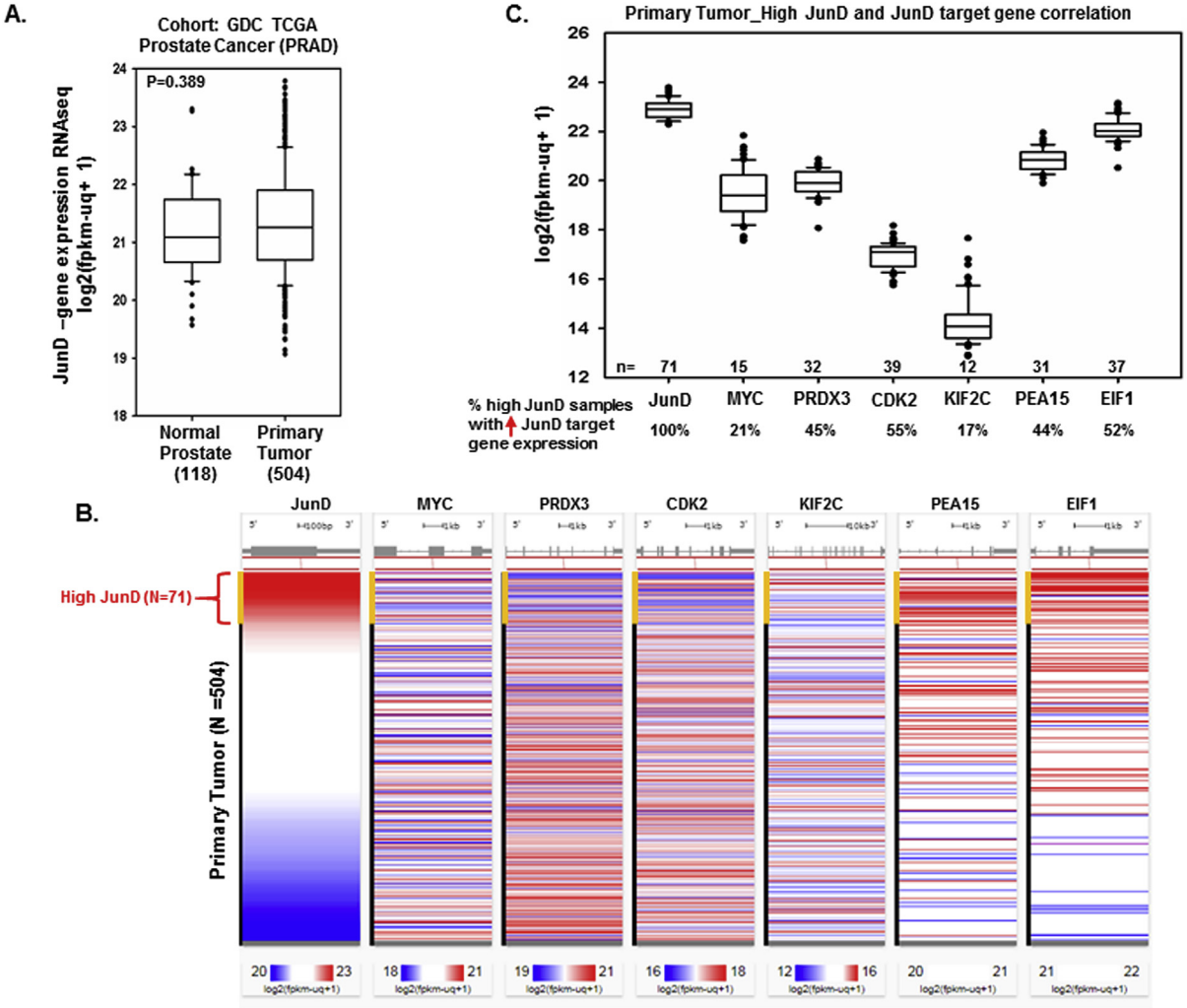


**Fig. 8. Analyzing JunD gene expression using The Cancer Genome Atlas (TCGA) Prostate Cancer samples.** ***A.*** The expression levels (RNA-seq data) of JunD in normal prostate tissues compared with human prostate cancer (primary tumors) in TCGA database. Significance was determined using one-way ANOVA. ***B.*** The expression levels of selected JunD dependent genes (MYC, PRDX3, CDK2, KIF2C, PEA15, and EIF1) were examined in primary tumor samples with high JunD levels (n = 71), indicated by the red color. ***C.*** Box plot showing the percentage (%) of high JunD primary tumors that also exhibited an increase in specific JunD dependent gene expression. (For interpretation of the references to color in this figure legend, the reader is referred to the Web version of this article.)

FOS family members, are well known for their involvement in almost all areas of eukaryotic cellular behavior from cell proliferation, differentiation to apoptosis [28,29,64,65]. Formation of the dimeric complex between AP-1 family members determines which genes are transcribed and the biological functions that are carried out [1,33,65,66]. Regarding the cell cycle, it is a well-established pathway mainly dependent on cyclin-dependent kinases (CDKs) which are positively regulated by cyclins and negatively regulated by cyclin-dependent kinase inhibitors (CKIs) [66,67]. Studies show that upon stimulation, JUN family members exhibit a rapid upregulation that effectively stimulates transcription of genes essential for entry into the G1 and S phases of the cell cycle such as the cyclins including cyclin D1, cyclin A, and cyclin E [64,66,68]. Likewise, the inhibition of several AP-1 family members depending on the context of a cell, results in a decrease in cyclins expression and cell growth inhibition [35,66,69]. Consistent with previous studies, we show that JunD down-regulation results in a significant decrease in many key players involved in cell cycle regulation including CDK1, CDK2, and CDK4 [41,70,71].

AP-1 proteins are also known to be involved in transformation and have been associated with aggressive clinical outcome in PCa [33,35]. The over-expression of JUN family members has been noted in several aggressive cancers including breast [27,72], lymphoma [73], colorectal adenocarcinoma [74], and PCa [33,64]. In line with these findings, we previously reported that JunD protein levels were remarkably higher in more aggressive PCa cell lines compared to normal prostate epithelial cells [29]. It has also been suggested by several studies that JUN activation is a crucial contributing factor for transformation and tumorigenesis, rather than an indirect effect on oncogenesis [64,65].

Along with AP-1 proteins, c-MYC is well-established as a significant driver of tumorigenesis in PCa [36–40]. Its over-expression in prostate tumors correlate with increased disease severity [39]. c-MYC has been implicated in all stages of disease progression, from the early phases of PCa development showing an overexpression of c-MYC mRNA and protein in prostatic intraepithelial neoplasia (PIN) as well as in primary human clinical PCa lesions to high-grade PIN lesions, which are precursors to many prostatic adenocarcinomas [11,36,37]. c-MYC regulates genes that are generally involved in cell cycle progression, which include CDKs [41,70,71,75]. c-MYC downregulation results in the inhibition of cell proliferation and cell cycle arrest at G2/M phase, which are associated with decreased expression of cyclins [76]. Although several studies indicate c-MYC as the regulator of cell cycle/proliferation, our reports suggest JunD as the critical player in cell proliferation, cell cycle regulation, and regulating several genes involved in cell cycle control including c-MYC [29]. The prerequisite for TFs to directly

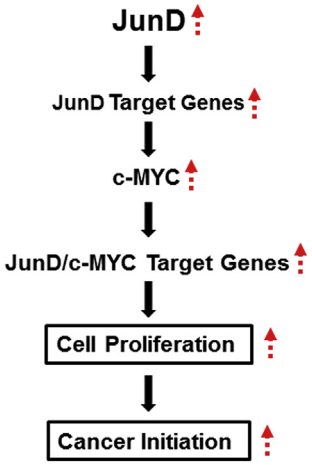


**Fig. 9. Proposed model for JunD mediated carcinogenesis in prostate cancer cells.** Schematic model indicating that JunD activates its dependent genes (JunD target genes), whose products target c-MYC which then leads to the activation of downstream targets (JunD/c-MYC target genes) that in turn induce cell proliferation of prostate cancer cells and carcinogenesis.

interact and regulate genes, is that an individual gene must have a response element in its promoter region that is recognized by that specific TF. JunD has previously been shown to bind to c-MYC promoter region through AP-1 response element (TGAGTCAG) and regulate c-MYC expression [77]. This may explain our findings where our data show that JunD overexpression increases c-MYC protein levels and ultimately an increase in cell proliferation (Fig. 6A and B). AP-1 activity is not only regulated as a result of the formation of a particular AP-1/DNA complex, but also via interacting with other signaling pathways such as NFKB, MAPK, or PI3K [1,78]. AP-1 family members can form complexes with a variety of other TFs to carry out several biological functions. AP-1 binding sites are present in the promotor region of Cyclin $D_1$, a known AP-1 target gene involved in cell cycle progression and is regulated by AP-1 [66,78]. Similarly, Cyclin $D_1$ is also regulated by c-MYC [41,70], suggesting a possible co-regulation by both AP-1 and c-MYC to induce cell cycle progression. Physical interactions between JunD and JunD-dependent genes, can be determined using chromatin immunoprecipitation (ChIP) to confirm target genes in continued studies.

We also confirmed regulation of additional cell cycle regulatory genes by JunD. We demonstrated in JunD-deficient cells that c-MYC, among other required proteins of cell cycle regulation including PRDX3 and CDK2, exhibited a decrease in its protein levels, while the overexpression of JunD enhanced their protein levels thereby supporting the increase of cell proliferation in PCa cells. Based on genomic studies from NCBI GEO datasets (https://www.ncbi.nlm.nih.gov/gds), PRDX3 [79,80], PEA15 [79,81], and KIF2C [79,82,83] were found to be highly expressed during PCa progression and in advanced metastatic PCa patient tissue samples compared to normal prostate tissues indicating their clinical relevance to cancer progression. Contradictory to these findings, using the TCGA database, there was no significant differences in JunD mRNA levels between normal and prostate cancer patient tissue samples. Although JunD RNA levels did not change, based on our transcriptomic and proteomic data from this study, RNA does not necessarily represent the abundance of protein. No previous studies have investigated these differences and it would be interesting to see how JunD protein levels in prostate cancer tissue samples correlate with JunD-dependent genes identified in this study.

As MYC is activated by several upstream oncogenic signaling pathways, we demonstrated that JunD-dependent genes require MYC signaling even in the presence of JunD by treating JunD overexpressing (D1) cells with JQ1, a small molecular inhibitor that targets c-MYC [57]. JQ1 has been shown in many studies to selectively down-regulate c-MYC transcription, deplete chromatin-bound c-MYC with a down-regulation of MYC-dependent target genes, and growth inhibition [56,57,84]. We observed that JQ1 treatment significantly decreased c-MYC, PRDX3, KIF2C, and CDK2 protein levels and inhibited JunD-mediated cell proliferation in PCa cells. Because CDK2 is a positive regulator of the cell cycle progression and represents a critical downstream mediator of c-MYC-induced regulation of cellular proliferation [41,70], our findings suggest that JunD-mediated cell proliferation and the expression of JunD-dependent genes rely on MYC signaling.

MYC can be activated by multiple mechanisms in cancer cells including transcriptional regulation, mRNA stabilization, and protein overexpression and stabilization [85]. Studies have demonstrated MYC's regulation in cancers by long noncoding RNAs (lncRNAs) [85,86], microRNAs (miRNAs) [87], and by TFs [88,89]. In line with these findings, our study also show that JunD deregulated genes were identified to be involved in some of the top mechanistic networks (according to IPA) including RNA processing (DIMT1, EFTUD2, HTT, PNN, RPS6/7, PTBP1, RRP1B, and SNRPD1), translational control (EIF1, EIF2AK2, ILF3, RPS5, and ANAX2), and protein stability (HSPA8, DNAJA1, USP15, XIAP, NEDD4, and ANAPC2). Further studies are needed to understand the regulation of c-MYC by JunD at different levels. A key question is how does JunD mediate its effects on c-MYC protein to carry out cell proliferation and ultimately PCa progression? One possibility is that the overexpression of JunD directly activates its target genes, whose products target c-MYC, thereby leading to an increase in c-MYC protein levels which then leads to the activation of downstream targets (JunD/c-MYC target genes) (Fig. 9). This cascade of events leads to the increase in cell proliferation of PCa cells and the initiation of carcinogenesis (Fig. 9).

Overall, these results show that JunD is essential for PCa cell proliferation, required for the expression of cell cycle-related genes, and it acts up-stream of c-MYC which is currently recognized as a significant factor in the initiation of prostate carcinogenesis. Although the majority of research reports related to c-MYC focused primarily on its normal physiological functions as well as its overexpression leading to carcinogenesis, our study shed light on possible mechanisms involved in upstream regulation of c-MYC by JunD. Our data also identified promising JunD target genes that may be required for the upregulation of c-MYC protein levels and also genes that function downstream c-MYC, such as PRDX3 to promote PCa. Identification of JunD target genes followed by the development of approaches to inhibit their expression and function will lead to the development of therapeutic and chemopreventive strategies to interfere with deregulation of cell proliferation and early stages of carcinogenesis.

## Conflicts of interest

The authors declare no conflict of interest.

## Availability of data

Microarray and Proteomics data were deposited into the GEO database. The accession number for the super series, which contains both microarray and proteomics datasets is https://www.ncbi.nlm.nih.gov/geo/query/acc.cgi?acc=GSE118123.

## Acknowledgements

This work was supported by the National Institutes of Health grant numbers 5G12MD007590 and 2P20MD002285; and by Spelman College's MBRS/RISE grant number 2R25GM060566-09A1 that supported the research training of undergraduate students V.E. and G.W. We are grateful to Dr. Chunliang Li from St. Jude Children's Research Hospital, Memphis TN, for kindly providing the "all in one-WT Cas 9" plasmid vector to generate the JunD KO prostate cancer cells in this study. We are also grateful to Santa Cruz for providing several free

antibodies samples for this study.

## Appendix A. Supplementary data

Supplementary data to this article can be found online at https://doi.org/10.1016/j.canlet.2019.02.005.

## References


[1] L.F. Zerbini, J.F. de Vasconcellos, A. Czibere, Y. Wang, J.D. Paccez, X. Gu, J.R. Zhou, T.A. Libermann, JunD-mediated repression of GADD45alpha and gamma regulates escape from cell death in prostate cancer, Cell Cycle 10 (2011) 2583–2591.

[2] R. Eeles, H. Ni Raghallaigh, Men with a susceptibility to prostate cancer and the role of genetic based screening, Transl. Androl. Urol. 7 (2018) 61–69.

[3] S.H. Tan, G. Petrovics, S. Srivastava, Prostate cancer genomics: recent advances and the prevailing underrepresentation from racial and ethnic minorities, Int. J. Mol. Sci. 19 (2018).

[4] D.W. Sonnenburg, A.K. Morgans, Emerging therapies in metastatic prostate cancer, Curr. Oncol. Rep. 20 (2018) 46.

[5] M. Kronig, C. Haverkamp, A. Schulte, L. Heinicke, K. Schaal, V. Drendel, M. Werner, U. Wetterauer, W. Schultze-Seemann, C.A. Jilg, Diabetes and beta-adrenergic blockage are risk factors for metastatic prostate cancer, World J. Surg. Oncol. 15 (2017) 50.

[6] A.K. Morgans, Y.H. Chen, C.J. Sweeney, D.F. Jarrard, E.R. Plimack, B.A. Gartrell, M.A. Carducci, M. Hussain, J.A. Garcia, D. Cella, R.S. DiPaola, L.J. Patrick-Miller, Quality of life during treatment with chemohormonal therapy: analysis of E3805 chemohormonal androgen ablation randomized trial in prostate cancer, J. Clin. Oncol.: Off. J. Am. Soc. Clin. Oncol. 36 (2018) 1088–1095.

[7] E. Scott, Chemohormonal therapy in metastatic hormone-sensitive prostate cancer, Sweeney CJ, Chen YH, Carducci M, Liu G, Jarrard DF, Eisenberger M, Wong YN, Hahn N, Kohli M, Cooney MM, Dreicer R, Vogelzang NJ, Picus J, Shevrin D, Hussain M, Garcia JA, DiPaola RS. Department of Medicine; Department of Biostatistics and Computational Biology; Dana-Farber Cancer Institute, Boston; Harvard Medical School, Boston; Johns Hopkins University, Baltimore; University of Wisconsin Carbone Cancer Center; School of Medicine and Public Health; Madison; Fox Chase Cancer Center, Temple University Health System, Philadelphia; Indiana University Melvin and Bren Simon Cancer Center, Indianapolis; Mayo Clinic, Rochester, MN; University Hospitals Case Medical Center, Seidman Cancer Center; Cleveland Clinic Taussig Cancer Institute; Both in Cleveland; University of Virginia Cancer Center, Charlottesville; Comprehensive Cancer Centers of Nevada, Las Vegas; Siteman Cancer Center, Washington University School of Medicine, St. Louis; NorthShore University Health System, Evanston, IL; University of Michigan Comprehensive Cancer Center, Ann Arbor; Rutgers cancer Institute of New Jersey, new Brunswick. N Engl J Med. 2015 Aug 20;373(8):737-746. [Epub 2015 Aug 5]. doi: 10.1056/NEJMoa1503747, Urol. Oncol. 35 (2017) 123.

[8] G. Schepisi, A. Farolfi, V. Conteduca, F. Martignano, D. De Lisi, G. Ravaglia, L. Rossi, C. Menna, S.R. Bellia, D. Barone, R. Gunelli, U. De Giorgi, Immunotherapy for prostate cancer: where we are headed, Int. J. Mol. Sci. 18 (2017).

[9] D. Gasi Tandefelt, J. Boormans, K. Hermans, J. Trapman, ETS fusion genes in prostate cancer, Endocr. Relat. Cancer 21 (2014) R143–R152.

[10] A. Ugalde-Olano, A. Egia, S. Fernandez-Ruiz, A. Loizaga-Iriarte, P. Zuniga-Garcia, S. Garcia, F. Royo, I. Lacasa-Viscasillas, E. Castro, A.R. Cortazar, A. Zabala-Letona, N. Martin-Martin, A. Arruabarrena-Aristorena, V. Torrano-Moya, L. Valcarcel-Jimenez, P. Sanchez-Mosquera, A. Caro-Maldonado, J. Gonzalez-Tampan, G. Cachi-Fuentes, E. Bilbao, R. Montero, S. Fernandez, E. Arrieta, K. Zorroza, M. Castillo-Martin, V. Serra, E. Salazar, N. Macias-Camara, J. Tabernero, J. Baselga, C. Cordon-Cardo, A.M. Aransay, A.D. Villar, J.L. Iovanna, J.M. Falcon-Perez, M. Unda, R. Bilbao, A. Carracedo, Methodological aspects of the molecular and histological study of prostate cancer: focus on PTEN, Methods 77–78 (2015) 25–30.

[11] T. Iwata, D. Schultz, J. Hicks, G.K. Hubbard, L.N. Mutton, T.L. Lotan, C. Bethel, M.T. Lotz, S. Yegnasubramanian, W.G. Nelson, C.V. Dang, M. Xu, U. Anele, C.M. Koh, C.J. Bieberich, A.M. De Marzo, MYC overexpression induces prostatic intraepithelial neoplasia and loss of Nkx3.1 in mouse luminal epithelial cells, PLoS One 5 (2010) e9427.

[12] R.J. Rebello, R.B. Pearson, R.D. Hannan, L. Furic, Therapeutic approaches targeting MYC-driven prostate cancer, Genes (2017) 8.

[13] C.R. Bethel, D. Faith, X. Li, B. Guan, J.L. Hicks, F. Lan, R.B. Jenkins, C.J. Bieberich, A.M. De Marzo, Decreased NKX3.1 protein expression in focal prostatic atrophy, prostatic intraepithelial neoplasia, and adenocarcinoma: association with gleason score and chromosome 8p deletion, Cancer Res. 66 (2006) 10683–10690.

[14] J.L. Merrimen, A.J. Evans, J.R. Srigley, Preneoplasia in the prostate gland with emphasis on high grade prostatic intraepithelial neoplasia, Pathology 45 (2013) 251–263.

[15] R. Montironi, R. Mazzucchelli, A. Lopez-Beltran, M. Scarpelli, L. Cheng, Prostatic intraepithelial neoplasia: its morphological and molecular diagnosis and clinical significance, BJU Int. 108 (2011) 1394–1401.

[16] I.H. Gelman, J. Peresie, K.H. Eng, B.A. Foster, Differential requirement for Src family tyrosine kinases in the initiation, progression, and metastasis of prostate cancer, Mol. Canc. Res. 12 (2014) 1470–1479.

[17] D.E. Linn, X. Yang, F. Sun, Y. Xie, H. Chen, R. Jiang, H. Chen, S. Chumsri, A.M. Burger, Y. Qiu, A role for OCT4 in tumor initiation of drug-resistant prostate cancer cells, Genes Cancer 1 (2010) 908–916.

[18] Q. Xie, Z.A. Wang, Transcriptional regulation of the Nkx3.1 gene in prostate luminal stem cell specification and cancer initiation via its 3' genomic region, J. Biol. Chem. 292 (2017) 13521–13530.

[19] H. Pan, Y. Zhu, W. Wei, S. Shao, X. Rui, Transcription factor FoxM1 is the downstream target of c-Myc and contributes to the development of prostate cancer, World J. Surg. Oncol. 16 (2018) 59.

[20] N. Selvaraj, J.A. Budka, M.W. Ferris, J.P. Plotnik, P.C. Hollenhorst, Extracellular signal-regulated kinase signaling regulates the opposing roles of JUN family transcription factors at ETS/AP-1 sites and in cell migration, Mol. Cell Biol. 35 (2015) 88–100.

[21] J.L. Robinson, K.S. Tzou, A.S. Parker, M.G. Heckman, K.J. Wu, T.W. Hilton, T.M. Pisansky, S.E. Schild, J.L. Peterson, L.A. Vallow, S.J. Buskirk, GATA2 expression and biochemical recurrence following salvage radiation therapy for relapsing prostate cancer, Br. J. Radiol. 90 (2017) 20170174.

[22] V. Rodriguez-Bravo, M. Carceles-Cordon, Y. Hoshida, C. Cordon-Cardo, M.D. Galsky, J. Domingo-Domenech, The role of GATA2 in lethal prostate cancer aggressiveness, Nature reviews, Urology 14 (2017) 38–48.

[23] C.S. Foster, A. Falconer, A.R. Dodson, A.R. Norman, N. Dennis, A. Fletcher, C. Southgate, A. Dowe, D. Dearnaley, S. Jhavar, R. Eeles, A. Feber, C.S. Cooper, Transcription factor E2F3 overexpressed in prostate cancer independently predicts clinical outcome, Oncogene 23 (2004) 5871–5879.

[24] S.J. Libertini, H. Chen, B. al-Bataina, T. Koilvaram, M. George, A.C. Gao, M. Mudryj, The interleukin 6 receptor is a direct transcriptional target of E2F3 in prostate tumor derived cells, Prostate 72 (2012) 649–660.

[25] K. Milde-Langosch, H. Roder, B. Andritzky, B. Aslan, G. Hemminger, A. Brinkmann, C.M. Bamberger, T. Loning, A.M. Bamberger, The role of the AP-1 transcription factors c-Fos, FosB, Fra-1 and Fra-2 in the invasion process of mammary carcinomas, Breast Canc. Res. Treat. 86 (2004) 139–152.

[26] P. Angel, M. Karin, The role of Jun, Fos and the AP-1 complex in cell-proliferation and transformation, Biochim. Biophys. Acta 1072 (1991) 129–157.

[27] A. Kharman-Biz, H. Gao, R. Ghiasvand, C. Zhao, K. Zendehdel, K. Dahlman-Wright, Expression of activator protein-1 (AP-1) family members in breast cancer, BMC Canc. 13 (2013) 441.

[28] R. Eferl, E.F. Wagner, AP-1: a double-edged sword in tumorigenesis, Nat. Rev. Canc. 3 (2003) 859–868.

[29] A.C. Millena, B.T. Vo, S.A. Khan, JunD is required for proliferation of prostate cancer cells and plays a role in transforming growth factor-beta (TGF-beta)-induced inhibition of cell proliferation, J. Biol. Chem. 291 (2016) 17964–17976.

[30] C.S. Barrett, A.C. Millena, S.A. Khan, TGF-beta effects on prostate cancer cell migration and invasion require FosB, Prostate 77 (2017) 72–81.

[31] C.C. Hsu, C.D. Hu, Transcriptional activity of c-Jun is critical for the suppression of AR function, Mol. Cell. Endocrinol. 372 (2013) 12–22.

[32] A. Hubner, D.J. Mulholland, C.L. Standen, M. Karasarides, J. Cavanagh-Kyros, T. Barrett, H. Chi, D.L. Greiner, C. Tournier, C.L. Sawyers, R.A. Flavell, H. Wu, R.J. Davis, JNK and PTEN cooperatively control the development of invasive adenocarcinoma of the prostate, Proc. Natl. Acad. Sci. U. S. A 109 (2012) 12046–12051.

[33] X. Ouyang, W.J. Jessen, H. Al-Ahmadie, A.M. Serio, Y. Lin, W.J. Shih, V.E. Reuter, P.T. Scardino, M.M. Shen, B.J. Aronow, A.J. Vickers, W.L. Gerald, C. Abate-Shen, Activator protein-1 transcription factors are associated with progression and recurrence of prostate cancer, Cancer Res. 68 (2008) 2132–2144.

[34] J. Edwards, N.S. Krishna, R. Mukherjee, J.M. Bartlett, The role of c-Jun and c-Fos expression in androgen-independent prostate cancer, J. Pathol. 204 (2004) 153–158.

[35] R. Kajanne, P. Miettinen, M. Tenhunen, S. Leppa, Transcription factor AP-1 promotes growth and radioresistance in prostate cancer cells, Int. J. Oncol. 35 (2009) 1175–1182.

[36] B. Gurel, T. Iwata, C.M. Koh, R.B. Jenkins, F. Lan, C. Van Dang, J.L. Hicks, J. Morgan, T.C. Cornish, S. Sutcliffe, W.B. Isaacs, J. Luo, A.M. De Marzo, Nuclear MYC protein overexpression is an early alteration in human prostate carcinogenesis, Mod. Pathol. 21 (2008) 1156–1167.

[37] K. Williams, S. Fernandez, X. Stien, K. Ishii, H.D. Love, Y.F. Lau, R.L. Roberts, S.W. Hayward, Unopposed c-MYC expression in benign prostatic epithelium causes a cancer phenotype, Prostate 63 (2005) 369–384.

[38] D.R. Wonsey, K.I. Zeller, C.V. Dang, The c-Myc target gene PRDX3 is required for mitochondrial homeostasis and neoplastic transformation, Proc. Natl. Acad. Sci. U. S. A. 99 (2002) 6649–6654.

[39] C.M. Koh, C.J. Bieberich, C.V. Dang, W.G. Nelson, S. Yegnasubramanian, A.M. De Marzo, MYC and prostate cancer, Genes Cancer 1 (2010) 617–628.

[40] D.M. Miller, S.D. Thomas, A. Islam, D. Muench, K. Sedoris, c-Myc and cancer metabolism, Clin. Cancer Res. 18 (2012) 5546–5553.

[41] M.K. Mateyak, A.J. Obaya, J.M. Sedivy, c-Myc regulates cyclin D-Cdk4 and -Cdk6 activity but affects cell cycle progression at multiple independent points, Mol. Cell Biol. 19 (1999) 4672–4683.

[42] A.J. Obaya, M.K. Mateyak, J.M. Sedivy, Mysterious liaisons: the relationship between c-Myc and the cell cycle, Oncogene 18 (1999) 2934–2941.

[43] L. Fan, G. Peng, N. Sahgal, L. Fazli, M. Gleave, Y. Zhang, A. Hussain, J. Qi, Regulation of c-Myc expression by the histone demethylase JMJD1A is essential for prostate cancer cell growth and survival, Oncogene 35 (2016) 2441–2452.

[44] S. Caggia, H. Chunduri, A.C. Millena, J.N. Perkins, S.V. Venugopal, B.T. Vo, C. Li, Y. Tu, S.A. Khan, Novel role of Gialpha2 in cell migration: downstream of PI3-kinase-AKT and Rac1 in prostate cancer cells, J. Cell. Physiol. 234 (2018) 802–815.

[45] B.T. Vo, C. Li, M.A. Morgan, I. Theurillat, D. Finkelstein, S. Wright, J. Hyle, S.M.C. Smith, Y. Fan, Y.D. Wang, G. Wu, B.A. Orr, P.A. Northcott, A. Shilatifard, C.J. Sherr, M.F. Roussel, Inactivation of Ezh2 upregulates Gfi1 and drives aggressive myc-driven group 3 medulloblastoma, Cell Rep. 18 (2017) 2907–2917.

[46] B. Elliott, D.L. Zackery, V.A. Eaton, R.T. Jones, F. Abebe, C.C. Ragin, S.A. Khan, Ethnic differences in TGFbeta-signaling pathway may contribute to prostate cancer health disparity, Carcinogenesis 39 (2018) 546–555.
[47] L. Walker, A.C. Millena, N. Strong, S.A. Khan, Expression of TGFbeta3 and its effects on migratory and invasive behavior of prostate cancer cells: involvement of PI3-kinase/AKT signaling pathway, Clin. Exp. Metastasis 30 (2013) 13–23.
[48] L.N. Lili, L.V. Matyunina, L.D. Walker, S.L. Wells, B.B. Benigno, J.F. McDonald, Molecular profiling supports the role of epithelial-to-mesenchymal transition (EMT) in ovarian cancer metastasis, J. Ovarian Res. 6 (2013) 49.
[49] R. Mezencev, L.V. Matyunina, N. Jabbari, J.F. McDonald, Snail-induced epithelial-to-mesenchymal transition of MCF-7 breast cancer cells: systems analysis of molecular changes and their effect on radiation and drug sensitivity, BMC Canc. 16 (2016) 236.
[50] B.T. Vo, S.A. Khan, Expression of nodal and nodal receptors in prostate stem cells and prostate cancer cells: autocrine effects on cell proliferation and migration, Prostate 71 (2011) 1084–1096.
[51] M. Zhang, L.V. Matyunina, L.D. Walker, W. Chen, H. Xiao, B.B. Benigno, R. Wu, J.F. McDonald, Evidence for the importance of post-transcriptional regulatory changes in ovarian cancer progression and the contribution of miRNAs, Sci. Rep. 7 (2017) 8171.
[52] B. Thompson, L. Varticovski, S. Baek, G.L. Hager, Genome-wide chromatin landscape transitions identify novel pathways in early commitment to osteoblast differentiation, PLoS One 11 (2016) e0148619.
[53] C. Zhou, Q. Zhong, L.V. Rhodes, I. Townley, M.R. Bratton, Q. Zhang, E.C. Martin, S. Elliott, B.M. Collins-Burow, M.E. Burow, G. Wang, Proteomic analysis of acquired tamoxifen resistance in MCF-7 cells reveals expression signatures associated with enhanced migration, Breast Cancer Res. 14 (2012) R45.
[54] L.J. Burton, M. Rivera, O. Hawsawi, J. Zou, T. Hudson, G. Wang, Q. Zhang, L. Cubano, N. Boukli, V. Odero-Marah, Muscadine grape skin extract induces an unfolded protein response-mediated autophagy in prostate cancer cells: a TMT-based quantitative proteomic analysis, PLoS One 11 (2016) e0164115.
[55] T. Tian, M. Wang, Y. Zhu, W. Zhu, T. Yang, H. Li, S. Lin, C. Dai, Y. Deng, D. Song, N. Li, Z. Zhai, Z.J. Dai, Expression, clinical significance, and functional prediction of MNX1 in breast cancer, Mol. Ther. Nucleic Acids 13 (2018) 399–406.
[56] L. Wang, X. Wu, P. Huang, Z. Lv, Y. Qi, X. Wei, P. Yang, F. Zhang, JQ1, a small molecule inhibitor of BRD4, suppresses cell growth and invasion in oral squamous cell carcinoma, Oncol. Rep. 36 (2016) 1989–1996.
[57] J.E. Delmore, G.C. Issa, M.E. Lemieux, P.B. Rahl, J. Shi, H.M. Jacobs, E. Kastritis, T. Gilpatrick, R.M. Paranal, J. Qi, M. Chesi, A.C. Schinzel, M.R. McKeown, T.P. Heffernan, C.R. Vakoc, P.L. Bergsagel, I.M. Ghobrial, P.G. Richardson, R.A. Young, W.C. Hahn, K.C. Anderson, A.L. Kung, J.E. Bradner, C.S. Mitsiades, BET bromodomain inhibition as a therapeutic strategy to target c-Myc, Cell 146 (2011) 904–917.
[58] H.C. Whitaker, D. Patel, W.J. Howat, A.Y. Warren, J.D. Kay, T. Sangan, J.C. Marioni, J. Mitchell, S. Aldridge, H.J. Luxton, C. Massie, A.G. Lynch, D.E. Neal, Peroxiredoxin-3 is overexpressed in prostate cancer and promotes cancer cell survival by protecting cells from oxidative stress, Br. J. Canc. 109 (2013) 983–993.
[59] S. Haider, R. Pal, Integrated analysis of transcriptomic and proteomic data, Curr. Genom. 14 (2013) 91–110.
[60] J.M. Lemee, A. Clavreul, M. Aubry, E. Com, M. de Tayrac, J. Mosser, P. Menei, Integration of transcriptome and proteome profiles in glioblastoma: looking for the missing link, BMC Mol. Biol. 19 (2018) 13.
[61] L.E. Pascal, L.D. True, D.S. Campbell, E.W. Deutsch, M. Risk, I.M. Coleman, L.J. Eichner, P.S. Nelson, A.Y. Liu, Correlation of mRNA and protein levels: cell type-specific gene expression of cluster designation antigens in the prostate, BMC Genomics 9 (2008) 246.
[62] Q. Tian, S.B. Stepaniants, M. Mao, L. Weng, M.C. Feetham, M.J. Doyle, E.C. Yi, H. Dai, V. Thorsson, J. Eng, D. Goodlett, J.P. Berger, B. Gunter, P.S. Linseley, R.B. Stoughton, R. Aebersold, S.J. Collins, W.A. Hanlon, L.E. Hood, Integrated genomic and proteomic analyses of gene expression in Mammalian cells, Mol. Cell. Proteomics: MCP 3 (2004) 960–969.
[63] L. Sevilla, A. Zaldumbide, P. Pognonec, K.E. Boulukos, Transcriptional regulation of the bcl-x gene encoding the anti-apoptotic Bcl-xL protein by Ets, Rel/NFkappaB, STAT and AP1 transcription factor families, Histol. Histopathol. 16 (2001) 595–601.
[64] P. Lopez-Bergami, E. Lau, Z. Ronai, Emerging roles of ATF2 and the dynamic AP1 network in cancer, Nat. Rev. Canc. 10 (2010) 65–76.
[65] E. Shaulian, M. Karin, AP-1 in cell proliferation and survival, Oncogene 20 (2001) 2390–2400.
[66] L. Bakiri, D. Lallemand, E. Bossy-Wetzel, M. Yaniv, Cell cycle-dependent variations in c-Jun and JunB phosphorylation: a role in the control of cyclin D1 expression, EMBO J. 19 (2000) 2056–2068.
[67] X. He, H. Xiang, X. Zong, X. Yan, Y. Yu, G. Liu, D. Zou, H. Yang, CDK2-AP1 inhibits growth of breast cancer cells by regulating cell cycle and increasing docetaxel sensitivity in vivo and in vitro, Cancer Cell Int. 14 (2014) 130.
[68] M. Katabami, H. Donninger, F. Hommura, V.D. Leaner, I. Kinoshita, J.F. Chick, M.J. Birrer, Cyclin A is a c-Jun target gene and is necessary for c-Jun-induced anchorage-independent growth in RAT1a cells, J. Biol. Chem. 280 (2005) 16728–16738.
[69] L. Xu, H. Ning, L. Gu, Q. Wang, W. Lu, H. Peng, W. Cui, B. Ying, C.R. Ross, G.M. Wilson, L. Wei, W.S. Wold, J. Liu, Tristetraprolin induces cell cycle arrest in breast tumor cells through targeting AP-1/c-Jun and NF-kappaB pathway, Oncotarget 6 (2015) 41679–41691.
[70] Y. Yang, K. Xue, Z. Li, W. Zheng, W. Dong, J. Song, S. Sun, T. Ma, W. Li, c-Myc regulates the CDK1/cyclin B1 dependentG2/M cell cycle progression by histone H4 acetylation in Raji cells, Int. J. Mol. Med. 41 (2018) 3366–3378.
[71] P. Hydbring, A. Castell, L.G. Larsson, MYC Modulation Around the CDK2/p27/SKP2 Axis, Genes (Basel), (2017), p. 8.
[72] S. Langer, C.F. Singer, G. Hudelist, B. Dampier, K. Kaserer, U. Vinatzer, H. Pehamberger, C. Zielinski, E. Kubista, M. Schreibner, Jun and Fos family protein expression in human breast cancer: correlation of protein expression and clinicopathological parameters, Eur. J. Gynaecol. Oncol. 27 (2006) 345–352.
[73] X. Mao, G. Orchard, Abnormal AP-1 protein expression in primary cutaneous B-cell lymphomas, Br. J. Dermatol. 159 (2008) 145–151.
[74] H. Wang, M. Birkenbach, J. Hart, Expression of Jun family members in human colorectal adenocarcinoma, Carcinogenesis 21 (2000) 1313–1317.
[75] R. Vartanian, J. Masri, J. Martin, C. Cloninger, B. Holmes, N. Artinian, A. Funk, T. Ruegg, J. Gera, AP-1 regulates cyclin D1 and c-MYC transcription in an AKT-dependent manner in response to mTOR inhibition: role of AIP4/Itch-mediated JUNB degradation, Mol. Canc. Res.: MCR 9 (2011) 115–130.
[76] A. Song, J. Ye, K. Zhang, L. Sun, Y. Zhao, H. Yu, Lentiviral vector-mediated siRNA knockdown of c-MYC: cell growth inhibition and cell cycle arrest at G2/M phase in Jijoye cells, Biochem. Genet. 51 (2013) 603–617.
[77] C. Iavarone, A. Catania, M.J. Marinissen, R. Visconti, M. Acunzo, C. Tarantino, M.S. Carlomagno, C.B. Bruni, J.S. Gutkind, M. Chiariello, The platelet-derived growth factor controls c-myc expression through a JNK- and AP-1-dependent signaling pathway, J. Biol. Chem. 278 (2003) 50024–50030.
[78] F. Chang, L.S. Steelman, J.T. Lee, J.G. Shelton, P.M. Navolanic, W.L. Blalock, R.A. Franklin, J.A. McCubrey, Signal transduction mediated by the Ras/Raf/MEK/ERK pathway from cytokine receptors to transcription factors: potential targeting for therapeutic intervention, Leukemia 17 (2003) 1263–1293.
[79] S.Y. Wong, H. Haack, J.L. Kissil, M. Barry, R.T. Bronson, S.S. Shen, C.A. Whittaker, D. Crowley, R.O. Hynes, Protein 4.1B suppresses prostate cancer progression and metastasis, Proc. Natl. Acad. Sci. U. S. A 104 (2007) 12784–12789.
[80] H. Satake, K. Tamura, M. Furihata, T. Anchi, H. Sakoda, C. Kawada, T. Iiyama, S. Ashida, T. Shuin, The ubiquitin-like molecule interferon-stimulated gene 15 is overexpressed in human prostate cancer, Oncol. Rep. 23 (2010) 11–16.
[81] S. Varambally, J. Yu, B. Laxman, D.R. Rhodes, R. Mehra, S.A. Tomlins, R.B. Shah, U. Chandran, F.A. Monzon, M.J. Becich, J.T. Wei, K.J. Pienta, D. Ghosh, M.A. Rubin, A.M. Chinnaiyan, Integrative genomic and proteomic analysis of prostate cancer reveals signatures of metastatic progression, Cancer Cell 8 (2005) 393–406.
[82] Y.P. Yu, D. Landsittel, L. Jing, J. Nelson, B. Ren, L. Liu, C. McDonald, R. Thomas, R. Dhir, S. Finkelstein, G. Michalopoulos, M. Becich, J.H. Luo, Gene expression alterations in prostate cancer predicting tumor aggression and preceding development of malignancy, J. Clin. Oncol.: Off. J. Am. Soc. Clin. Oncol. 22 (2004) 2790–2799.
[83] U.R. Chandran, C. Ma, R. Dhir, M. Bisceglia, M. Lyons-Weiler, W. Liang, G. Michalopoulos, M. Becich, F.A. Monzon, Gene expression profiles of prostate cancer reveal involvement of multiple molecular pathways in the metastatic process, BMC Canc. 7 (2007) 64.
[84] F. Mao, J. Li, Q. Luo, R. Wang, Y. Kong, C. Carlock, Z. Liu, B.D. Elzey, X. Liu, Plk1 inhibition enhances the efficacy of BET epigenetic reader blockade in castration-resistant prostate cancer, Mol. Canc. Therapeut. 17 (2018) 1554–1565.
[85] Z. Wang, B. Yang, M. Zhang, W. Guo, Z. Wu, Y. Wang, L. Jia, S. Li, N. Cancer Genome Atlas Research, W. Xie, D. Yang, lncRNA epigenetic landscape analysis identifies EPIC1 as an oncogenic lncRNA that interacts with MYC and promotes cell-cycle progression in cancer, Cancer Cell 33 (2018) 706–720 e709.
[86] J.R. Prensner, W. Chen, S. Han, M.K. Iyer, Q. Cao, V. Kothari, J.R. Evans, K.E. Knudsen, M.T. Paulsen, M. Ljungman, T.S. Lawrence, A.M. Chinnaiyan, F.Y. Feng, The long non-coding RNA PCAT-1 promotes prostate cancer cell proliferation through cMyc, Neoplasia 16 (2014) 900–908.
[87] K.B. Challagundla, X.X. Sun, X. Zhang, T. DeVine, Q. Zhang, R.C. Sears, M.S. Dai, Ribosomal protein L11 recruits miR-24/miRISC to repress c-Myc expression in response to ribosomal stress, Mol. Cell Biol. 31 (2011) 4007–4021.
[88] K.M. Scully, R. Lahmy, L. Signaevskaia, R. Sasik, R. Medal, H. Kim, R. French, B. James, Y. Wu, A.M. Lowy, P. Itkin-Ansari, E47 governs the MYC-CDKN1B/p27(KIP1)-RB network to growth arrest PDA cells independent of CDKN2A/p16(INK4A) and wild-type p53, Cell Mol Gastroenterol Hepatol 6 (2018) 181–198.
[89] X. Zhou, Y. Wen, Y. Tian, M. He, X. Ke, Z. Huang, Y. He, L. Liu, A. Scharf, M. Lu, G. Zhang, Y. Deng, Y. Yan, M.P. Mayer, X. Chen, F. Zou, Hsp90alpha-dependent Bclaf1 promotes hepatocellular carcinoma proliferation by regulating c-MYC mRNA stability, Hepatology 0 (0) (2018), https://doi.org/10.1002/hep.30172 Epub ahead of print.